

Design of Filtering Coupled-Line Trans-Directional Coupler with Broadband Bandpass Response

Hongmei Liu*, Xiaoting Li, Yongquan Guo, Shaojun Fang, and Zhongbao Wang

Abstract—In the paper, a filtering coupled-line trans-directional (CL-TRD) coupler with broadband bandpass response is presented for the first time. It is composed of three sections of coupled lines, four transmission lines, and four shunt stubs. Design equations of the proposed filtering CL-TRD coupler are derived using the even- and odd-mode analysis. For demonstration, a prototype operating at 2.4 GHz is designed, fabricated, and measured. Under the criterion of $|S_{11}| < -10$ dB, the measured bandpass bandwidth is 41.7%. In this bandwidth, the output port phase difference is within $90^\circ \pm 5^\circ$. Besides, two stopbands (0.91 GHz \sim 1.89 GHz and 3.36 GHz \sim 4.3 GHz) are obtained on both sides of the passband with sharp rejection. The measurements and comparisons results show that smaller size, wider bandwidth, and easier fabrication than the reported filtering couplers are exhibited by the proposed filtering CL-TRD coupler. It indicates that a good candidate for filtering-coupling applications can be served by the proposed coupler.

1. INTRODUCTION

Quadrature coupler is an important passive component for dividing or combining RF signals with a phase difference of 90° in various circuits such as balanced amplifier, antenna feeding network, and mixer [1, 2]. Bandpass filter is another essential component at the front-end of a typical RF system for distinguishing the desired signal from extraneous signals outside the targeted bands of interest [3, 4]. In general, filter and coupler are designed separately and cascaded connected, which will cause high insertion loss, degraded performance, and bulky circuit size. In order to improve the whole circuit performance and reduce size, filtering coupler has been recently receiving great attention.

In [5], a filtering rat-race coupler using dual-mode stub-loaded resonators (SLRs) is proposed with a bandpass bandwidth (BPBW) of 6.7%. In [6], a filtering branch-line coupler with resonators is proposed. It has a BPBW of 3.17%. In [7], a filtering 180° patch coupler with inset fed approach and proper port location is reported. The BPBW of 7.4% is obtained. In [8], a filtering 180° hybrid coupler with coupled resonators is introduced. It exhibits a BPBW of 5%. Although the couplers in [5–8] are integrated with functions of filtering, their BPBWs are all narrow ($< 8\%$).

To enhance the bandwidth, several techniques have been applied. In [9], a filtering branch-line coupler using coupled lines is presented. The BPBW is increased to 53%. By using stubs and sub-circuits, a filtering rat-race coupler with BPBW of 100% is introduced [10]. In [11], filtering couplers with bandpass and bandstop filters are proposed, which have the BPBW of 17%. In [12], a three-port filtering coupler with coupled lines and a phase shifter is designed. The measured BPBW is 51%. In [13], a filtering coupler is constructed with a coupled-multi-line filtering section. The 3-dB-referred absolute bandwidth of 13% is achieved. In [14], by using a coupled line structure, a filtering rat-race coupler with a BPBW of 32.5% is designed. In [15], a filtering 90° coupler using a stacked cross coupled-line and loaded cross-stub is proposed, which has a bandwidth of 53%. Although different

Received 4 November 2020, Accepted 7 January 2021, Scheduled 20 January 2021

* Corresponding author: Hongmei Liu (lhm323@dlmu.edu.cn).

The authors are with the School of Information Science and Technology, Dalian Maritime University, Dalian, Liaoning 116026, China.

technologies [9–15] are utilized to obtain wideband BPBW with filtering characteristic, they have similar disadvantages. For example, since these filtering couplers are based on branch lines or rat-race couplers, the circuit size is inherently large [9–11]. Most of the circuits use tight coupling coupled lines for wideband filtering, and the fabrication difficulty is increased [9, 10, 12–15]. Moreover, some circuit structures are complicated [10–15].

In general, depending on the relative locations of the isolated port to the input port, the quadrature couplers can be classified into three types, namely, co-directional, contra-directional, and trans-directional (TRD), as shown in Fig. 1. So far, most of the filtering couplers are based on branch-line couplers, which belong to the co-directional type. Since a branch-line coupler is composed of four transmission lines with $\lambda_0/4$ length, it has the inherent disadvantages of large size and narrow bandwidth. The contra-directional couplers are often constructed by parallel coupled lines, named as coupled-line contra-directional (CL-CTD) coupler. However, due to the limited production process, the gap of the coupled lines cannot be too small. So tight coupling (3–6 dB) cannot be achieved. The TRD coupler is constructed by capacitor loaded coupled lines, named as coupled-line trans-directional (CL-TRD) coupler [16]. Compared with a branch-line co-directional (BL-COD) coupler, a CL-TRD coupler shows wider bandwidth and smaller size. Compared with a CL-CTD coupler, a CL-TRD coupler can realize tight coupling easily. Besides, since the output ports of the CL-TRD coupler are on the same side of the coupled line, the connection with other devices is easier.

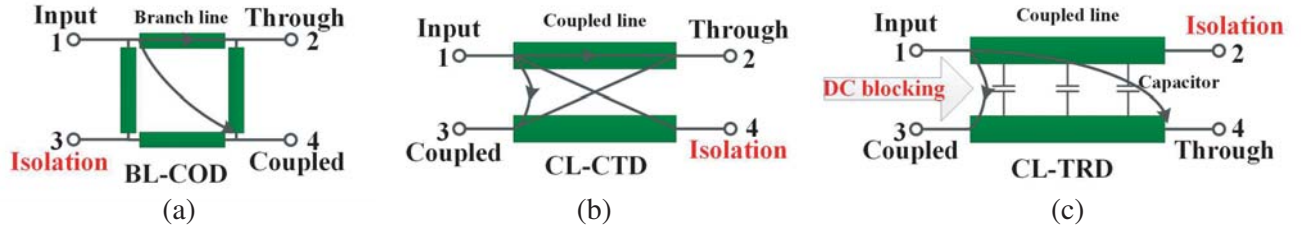


Figure 1. Three types of directional couplers. (a) Co-directional coupler. (b) Contra-directional coupler. (c) Trans-directional (TRD) coupler.

In the paper, a filtering CL-TRD coupler with broadband bandpass response is proposed for the first time. It is composed of three coupled lines, four transmission lines, and four shunt stubs. By using the shunt stubs, two transmission zeros are obtained. By inserting the transmission lines, additional resonant frequencies are created, resulting in wide passband. The analysis of the proposed filtering TRD coupler is introduced in Section 2. Section 3 shows the implementation of the designed prototype, followed by a conclusion in Section 4.

2. THEORETICAL ANALYSIS

Figure 2 shows the schematic of the proposed broadband filtering CL-TRD coupler. It consists of three coupled lines, four transmission lines, and four shunt stubs. The three coupled lines include two parallel coupled lines and one periodically capacitor loaded parallel coupled line. In the design, the period is set to 3, which means that three capacitors are shunt between the parallel coupled lines. The three coupled lines have the same even- and odd-mode characteristic impedances of Z_e and Z_o . The first and third coupled lines have the same electrical length of θ_4 . The second coupled line has an electrical length of θ_0 . Three capacitors, named as C_1 , are shunt between the middle of coupled lines. Let θ_2 and Z_2 be the electrical length and impedance of the shunt stubs, respectively. Let θ_3 and Z_3 denote the electrical length and impedance of the transmission lines, respectively. Without loss of generality, if port 1 is driven as the input port, ports 2, 3 and 4 are the isolation, coupling, and through port, individually.

Since the proposed circuit is doubly symmetry, even- and odd-mode analysis is used. Fig. 3 shows the even- and odd-mode sub-circuits of the proposed coupler. According to the transmission lines theory [17], the port impedances of the sub-circuits can be obtained. Equations (1)–(3) show the

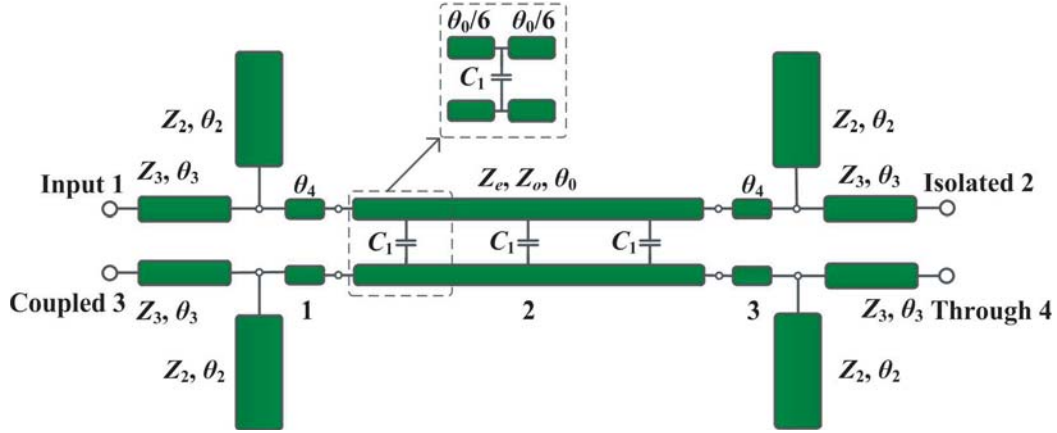


Figure 2. Schematic of the proposed filtering CL-TRD coupler.

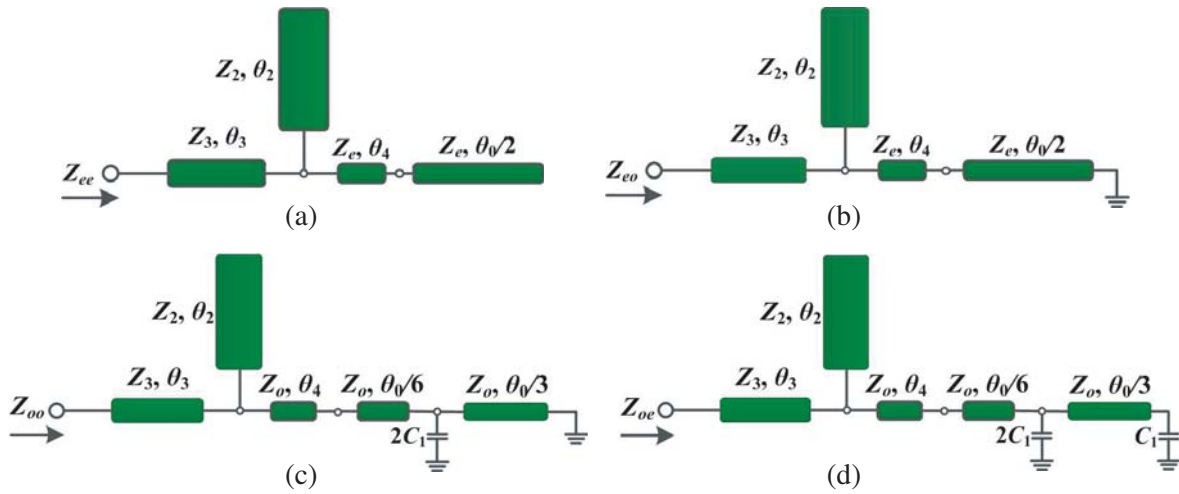


Figure 3. Equivalent even- and odd-mode circuits of the proposed coupler. (a) Even-even-mode. (b) Even-odd-mode. (c) Odd-odd-mode. (d) Odd-even-mode.

expressions of each port impedance.

$$Z_{ee} = j \left[\frac{Z_3^2 Y_2 N + Z_3^2 Y_e \tan(\theta_3) \tan\left(\frac{\theta_0}{2} + \theta_4\right) - Z_3}{\tan(\theta_3) + Z_3 Y_2 \tan(\theta_2) + Z_3 Y_e \tan\left(\frac{\theta_0}{2} + \theta_4\right)} \right] \quad (1a)$$

$$Z_{eo} = j \left[\frac{Z_3 Z_e \tan\left(\frac{\theta_0}{2} + \theta_4\right) + Z_3^2 (\tan(\theta_3) - Y_2 Z_e M)}{Z_3 - (Z_3 Y_2 \tan(\theta_2) + \tan(\theta_3)) Z_e \tan\left(\frac{\theta_0}{2} + \theta_4\right)} \right] \quad (1b)$$

$$Z_{oo} = \frac{Z_3 A_1 (1 - Z_3 Y_2 N) + j Z_3^2 \tan(\theta_3)}{Z_3 + j A_1 (\tan(\theta_3) + Z_3 Y_2 \tan(\theta_2))} \quad (1c)$$

$$Z_{oe} = \frac{Z_3 A_3 (1 - Z_3 Y_2 N) + j Z_3^2 \tan(\theta_3)}{Z_3 + j A_3 (\tan(\theta_3) + Z_3 Y_2 \tan(\theta_2))} \quad (1d)$$

where

$$N = \tan(\theta_2) \tan(\theta_3) \quad (2a)$$

$$M = \tan(\theta_2) \tan(\theta_3) \tan\left(\frac{\theta_0}{2} + \theta_4\right) \quad (2b)$$

$$A_1 = \frac{Z_o A_2 + j Z_o^2 \tan\left(\frac{\theta_0}{6} + \theta_4\right)}{Z_o + j A_2 \tan\left(\frac{\theta_0}{6} + \theta_4\right)} \quad (3a)$$

$$A_2 = \frac{j Z_o \tan\left(\frac{\theta_0}{3}\right)}{1 - 2\omega C_1 Z_o \tan\left(\frac{\theta_0}{3}\right)} \quad (3b)$$

$$A_3 = \frac{Z_o A_4 + j Z_o^2 \tan\left(\frac{\theta_0}{6} + \theta_4\right)}{Z_o + j A_4 \tan\left(\frac{\theta_0}{6} + \theta_4\right)} \quad (3c)$$

$$A_4 = j \frac{\omega C_1 Z_o^2 \tan\left(\frac{\theta_0}{3}\right) - Z_o}{3\omega C_1 Z_o + \tan\left(\frac{\theta_0}{3}\right) - 2\omega^2 C_1^2 Z_o^2 \tan\left(\frac{\theta_0}{3}\right)} \quad (3d)$$

According to [17], the S -parameters for a symmetrical four-port network can be expressed as below.

$$S_{11} = \frac{(\Gamma_{ee} + \Gamma_{oe}) + (\Gamma_{eo} + \Gamma_{oo})}{4} \quad (4a)$$

$$S_{21} = \frac{(\Gamma_{ee} + \Gamma_{oe}) - (\Gamma_{eo} + \Gamma_{oo})}{4} \quad (4b)$$

$$S_{31} = \frac{(\Gamma_{ee} - \Gamma_{oe}) - (\Gamma_{eo} - \Gamma_{oo})}{4} \quad (4c)$$

$$S_{41} = \frac{(\Gamma_{ee} - \Gamma_{oe}) + (\Gamma_{eo} - \Gamma_{oo})}{4} \quad (4d)$$

where

$$\Gamma_{i,j} = \frac{Z_{i,j} - Z_0}{Z_{i,j} + Z_0} \quad (i, j = e, o) \quad (5)$$

$\Gamma_{(e,o)}$ is reflection coefficient, $T_{(e,o)}$ the transmission coefficient, and Z_0 the reference impedance.

According to [16], the following conditions should be satisfied to operate as a TRD coupler.

$$|S_{11}| = |S_{21}| = 0 \quad (6a)$$

$$\frac{|S_{31}|}{|S_{41}|} = \frac{k}{\sqrt{1 - k^2}} \quad (6b)$$

where k is the coupling coefficient.

Substituting Eqs. (4) and (5) into Eq. (6), the following relations can be obtained.

$$Z_0^2 = Z_{ee} Z_{oe} \quad (7a)$$

$$Z_0^2 = Z_{eo} Z_{oo} \quad (7b)$$

$$\left| \frac{Z_0 (Z_{ee} - Z_{eo})}{Z_{ee} Z_{eo} - Z_0^2} \right| = \frac{k}{\sqrt{1 - k^2}} \quad (7c)$$

Substituting Eq. (1) into Eq. (7c), the expression of the even-mode characteristic impedance of the coupled line (Z_e) can be obtained, as shown in Equations (8)–(13).

$$Z_e = \frac{-B_0 \pm \left[B_0^2 - 4 \left(kZ_3 (Z_3 - B_1) \tan\left(\frac{\theta_1}{2}\right) + \sqrt{1-k^2} B_2 Z_3 Z_0 \tan\left(\frac{\theta_1}{2}\right) \right) \left(\sqrt{1-k^2} B_3 Z_3 Z_0 \tan\left(\frac{\theta_1}{2}\right) \right) \right]^{\frac{1}{2}}}{2 \left[kZ_3 (Z_3 - B_1) \tan\left(\frac{\theta_1}{2}\right) + \sqrt{1-k^2} B_2 Z_3 Z_0 \tan\left(\frac{\theta_1}{2}\right) \right]} \quad (8)$$

where

$$\theta_1 = \theta_0 + 2\theta_4 \quad (9)$$

$$B_0 = k \left[B_3 (Z_3 - B_1) - Z_0^2 \right] - \sqrt{1-k^2} Z_0 \left[B_1 \left(Z_3 - B_2 Z_e \tan\left(\frac{\theta_1}{2}\right) \right) - Z_3^2 \left(1 + \tan^2\left(\frac{\theta_1}{2}\right) \right) + B_2 Z_e \tan\left(\frac{\theta_1}{2}\right) Z_3 - B_2 B_3 \right] \quad (10)$$

$$B_1 = Z_3^2 \tan(\theta_3) \left(Y_2 \tan(\theta_2) + Y_e \tan\left(\frac{\theta_1}{2}\right) \right) \quad (11)$$

$$B_2 = Z_3 Y_2 \tan(\theta_2) + \tan(\theta_3) \quad (12)$$

$$B_3 = Z_3^2 \tan(\theta_3) \left(1 - Y_2 Z_e \tan(\theta_2) \tan\left(\frac{\theta_1}{2}\right) \right) \quad (13)$$

Substituting Eq. (1) into Eq. (7a), the expression of the odd-mode characteristic impedance of the coupled line (Z_o) can be obtained, as shown in Equations (14)–(17).

$$Z_o = \frac{-D_1 - jD_2 A_4 (1 - Z_0^2) \pm \left[(D_1 + jD_2 A_4 (1 - Z_0^2))^2 - j4 \tan^2\left(\frac{\theta_0}{6} + \theta_4\right) D_1 A_4 (D_3 - D_2) \right]^{\frac{1}{2}}}{2 \tan\left(\frac{\theta_0}{6} + \theta_4\right) (D_3 - D_2)} \quad (14)$$

where

$$D_1 = Z_3^2 (1 - B_1) \tan(\theta_3) - Z_0^2 Z_3 \left(B_2 + Z_3 Y_e \tan\left(\frac{\theta_1}{2}\right) \right) \quad (15)$$

$$D_2 = (1 - Z_3 Y_2 \tan(\theta_2) \tan(\theta_3)) (B_1 - Z_3) \quad (16)$$

$$D_3 = Z_0^2 (\tan(\theta_3) + Z_3 Y_2 \tan(\theta_2)) \left(B_2 + Z_3 Y_e \tan\left(\frac{\theta_1}{2}\right) \right) \quad (17)$$

According to Eqs. (8)–(13), it is found that Z_e can be a function of θ_1 with certain values of θ_3 , Z_3 , θ_2 and Z_2 . Based on Eqs. (14)–(17), it is found that Z_o can be a function of C_1 with fixed values of θ_3 , Z_3 , θ_2 , and Z_2 . Thus, the values of θ_3 , Z_3 , θ_2 , and Z_2 should be firstly determined, which means that the circuit parameters of the shunt stubs (Z_2 , θ_2) and the transmission lines (Z_3 , θ_3) should be considered. The shunt stubs are utilized to generate stopbands on the two sides of the passband, which has no influence on the passband. Thus, the value of θ_2 should be 180° corresponding to the passband center frequency. For achieving wider filtering stopbands, the value of Z_2 should be as small as possible. The transmission lines are used to generate two extra resonate frequencies for enhancing the passband bandwidth. For simplification, the transmission lines are assumed to have no effects on the performance of the center frequency. Thus, the value of θ_3 is chosen as 180° corresponding to the passband center frequency. The value of Z_3 can be determined by the desired passband bandwidth. In the following, a prototype is designed, and the procedures are given for convenience.

3. IMPLEMENTATION AND RESULTS

In this section, a 3-dB filtering CL-TRD coupler working at 2.4 GHz is designed. The procedures are as follows:

Step 1: Obtain the values of Z_e , θ_0 , and θ_4 .

Since the values of θ_2 and θ_3 should be 180° corresponding to the passband center frequency, they have no effects on the equations at the center frequency. According to Eqs. (8)-(13), the curve of Z_e versus θ_1 can be plotted, as shown in Fig. 4. It is observed that as θ_1 increases from 0° to 14° , the value of Z_e increases from $120.7\ \Omega$ to $170\ \Omega$. For easy fabrication, the value of Z_e is chosen as $135\ \Omega$, and the corresponding value of θ_1 is 120° . It is noted that θ_1 is the sum of electrical lengths of the two parallel coupled lines and one periodically capacitor loaded parallel coupled line. Here, the electrical length (θ) of the periodically capacitor loaded coupled line is assigned as 90° for easy calculation based on [16]. Thus, the value of θ_4 is 15° .

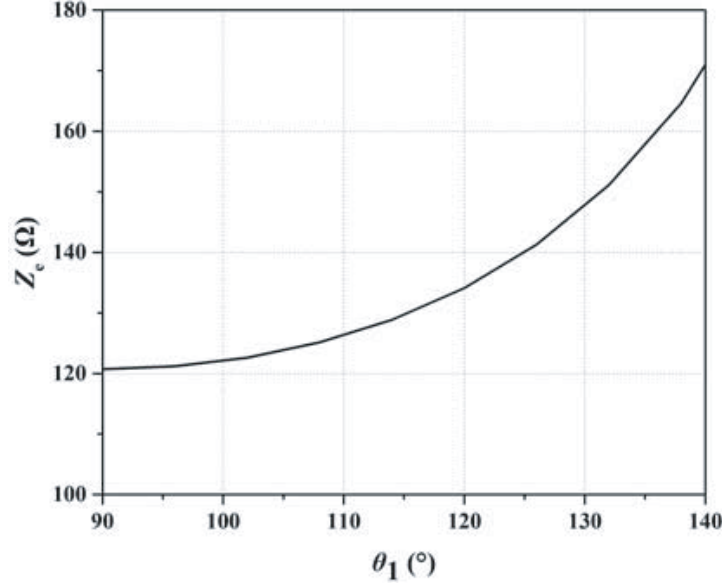


Figure 4. Curve of Z_e versus θ_4 .

Step 2: Obtain the values of Z_o , and C_1 .

According to Eqs. (14)–(16), the curve of Z_o versus C_1 can be plotted, as displayed in Fig. 5. It is observed that as C_1 increases from $1.25\ \text{pF}$ to $2.25\ \text{pF}$, the value of Z_o is decreased from $80\ \Omega$ to $40\ \Omega$. For easy fabrication of the coupled line, weak coupling ($> 6\ \text{dB}$) is preferred. Since Z_e is chosen as $135\ \Omega$, the value of Z_o should be more than $45\ \Omega$, corresponding to C_1 less than $2.1\ \text{pF}$. In this design, the value of C_1 is chosen as $1.5\ \text{pF}$, and the corresponding value of Z_o is $65\ \Omega$. The coupling of the coupled line is $9\ \text{dB}$.

Step 3: Obtain the values of Z_2 and Z_3 .

Since the value of θ_2 is 180° corresponding to the passband center frequency of $2.4\ \text{GHz}$, two stopbands at $1.2\ \text{GHz}$ and $3.6\ \text{GHz}$ can be obtained. For achieving wider filtering stopbands, the value of Z_2 should be as small as possible. After considering the fabrication limitations and size reduction, the value of Z_2 is chosen as $45\ \Omega$. The value of Z_3 is related to the passband bandwidth. Fig. 6 shows the curves of the $|S_{11}|$ versus different values of Z_3 . It is observed that different return loss curves can be achieved when Z_3 is varied from $60\ \Omega$ to $100\ \Omega$. For BPBW $> 40\%$ under the criterion of $|S_{11}| < -10\ \text{dB}$ and symmetry of the passband, the value of Z_3 is selected as $80\ \Omega$.

Table 1 shows the circuit parameters of the proposed filtering CL-TRD coupler. According to the

Table 1. The parameter values of the filtering CL-TRD coupler.

$Z_2(\Omega)$	$Z_3(\Omega)$	$Z_o(\Omega)$	$Z_e(\Omega)$	$\theta_2(^\circ)$	$\theta_3(^\circ)$	$\theta_e(^\circ)$	$\theta_o(^\circ)$	$C_1(\text{pF})$
45	80	65	135	180	180	90	90	1.5

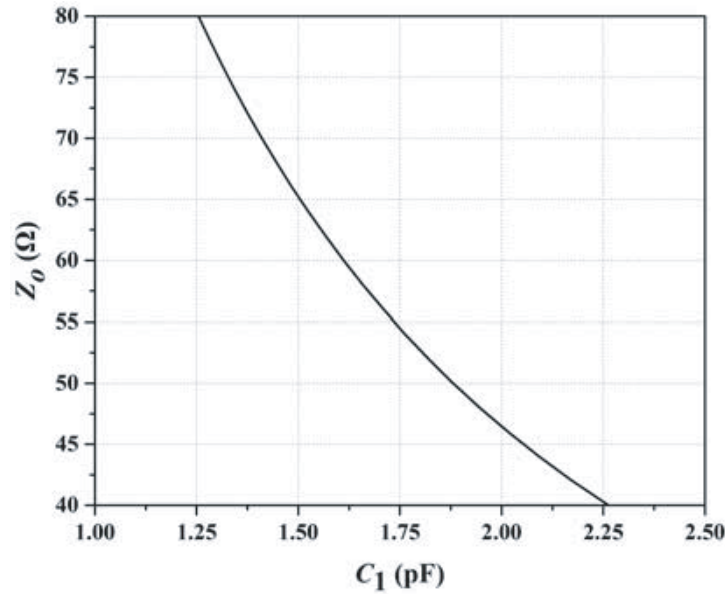


Figure 5. Curve of Z_0 versus C_1 .

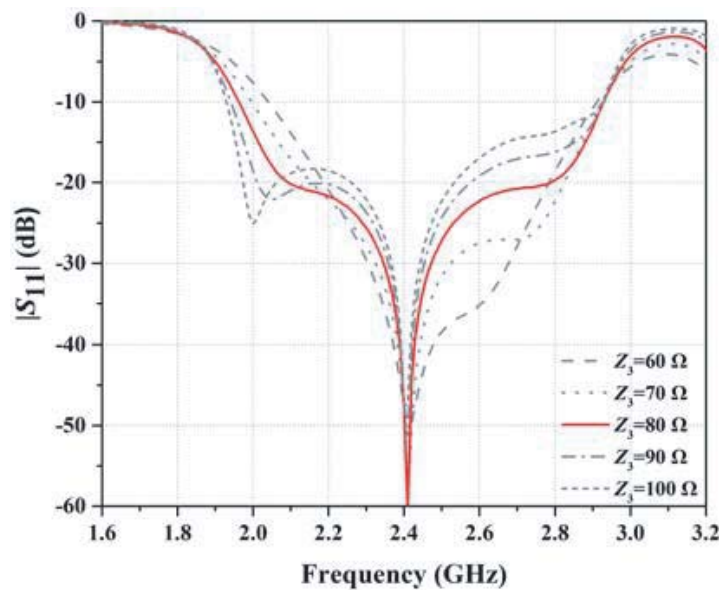


Figure 6. Curve of $|S_{11}|$ versus Z_3 .

design parameters, a simulation is carried out, and the calculated results are shown in Fig. 7. It is observed that under the criterion of $|S_{11}| < -10$ dB, the BPBW is from 1.97 GHz to 2.92 GHz. Within the passband, $|S_{21}|$ is below -13 dB. From 2.26 GHz to 2.87 GHz, the amplitude (AP) imbalance is less than 1 dB, and the phase difference is within $90^\circ \pm 5^\circ$. Besides, two stopbands (0.88 ~ 1.64 GHz and 3.32 ~ 4.18 GHz) with rapid out-of-band suppression are generated, which shows good bandpass filtering response.

Using an F4B substrate with dielectric constant $\epsilon_r = 3$, loss tangent $\delta = 0.003$, and thickness $h = 1.5$ mm, a prototype was fabricated. Fig. 8(a) shows the layout of the designed circuit. Since transmission lines and shunt stubs are included in the proposed circuit, the layout can be flexible in order to satisfy specific demands. To reduce size, the transmission lines and stubs are bent in

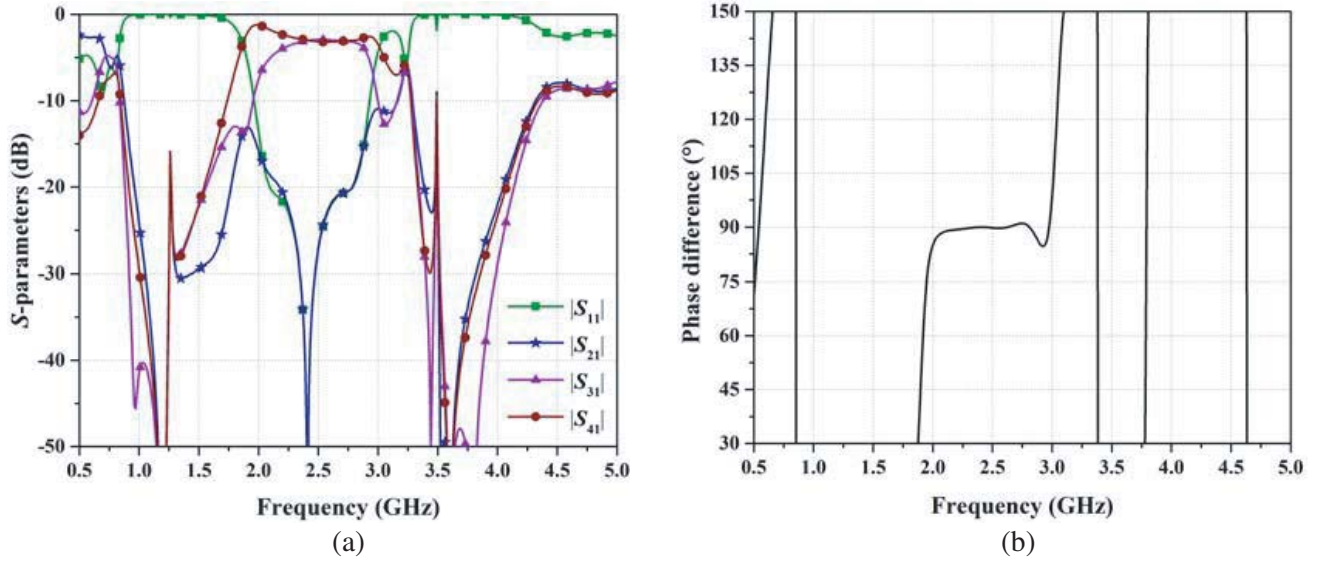


Figure 7. The simulation results of the schematic. (a) S -parameters. (b) Out ports phase difference.

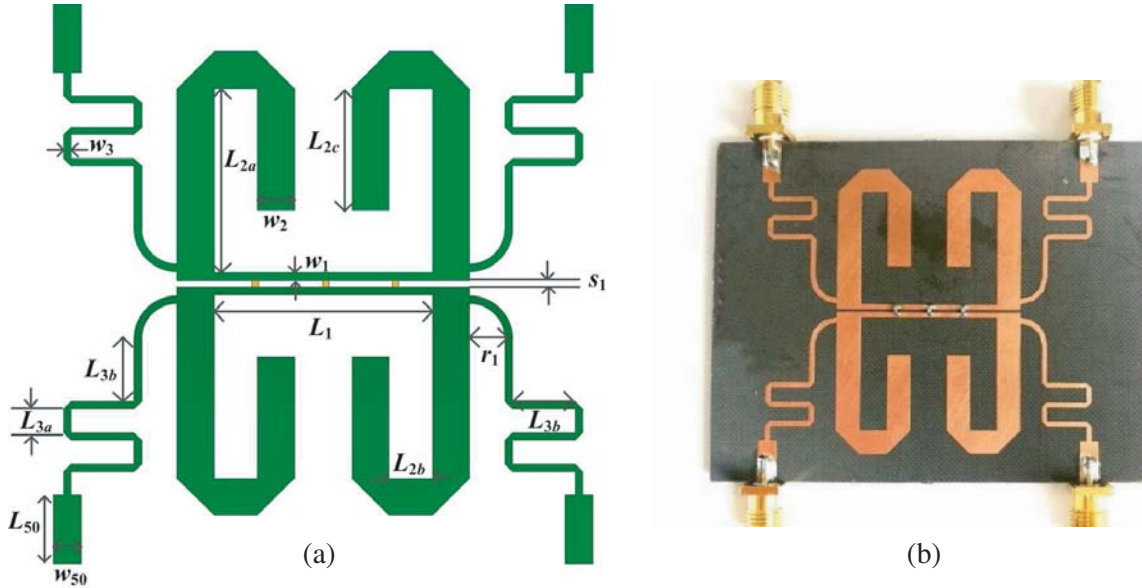


Figure 8. (a) The layout and (b) photograph of the filtering CL-TRD coupler.

the implementation. The lengths of L_{2a} , L_{2b} , and L_{2c} are assigned as $0.5\lambda_g$, $0.11\lambda_g$, and $0.39\lambda_g$, respectively (λ_g is the wavelength at the center frequency). The lengths of L_{3a} and L_{3b} are assigned as $0.07\lambda_g$ and $0.15\lambda_g$, respectively. According to Table 1, the initial dimensions can be calculated using the ADS *linecalc* software. Table 2 shows the calculated results. Based on the initial dimensions, the circuit is optimized by the Ansoft HFSS. Table 2 shows the final dimensions. It is observed that most of the optimized dimensions are similar to the calculated ones, which demonstrates the design equations. Fig. 8(b) shows a photograph of the fabricated circuit. The overall size of the circuit is $71.3\text{ mm} \times 51.7\text{ mm}$, which is corresponding to $0.88\lambda_g \times 0.64\lambda_g$. In the realization, three 1.6-pF (Murata, ERB1885C2E2R4CDX1) capacitors are soldered between the coupled lines to complete the TRD coupler.

The circuit is measured using Agilent N5230A network analyzer. Fig. 9 shows the simulated and

Table 2. The calculated and optimized dimensions of the prototype (Unit: mm).

	Calculated	Optimized		Optimized	Calculated
h	1.5	1.5	w_3	0.9	1.5
w_1	0.93	0.9	L_{3a}	2.4	2.7
s_1	0.45	0.5	L_{3b}	6.4	6.6
L_1	22.46	22.4	L_{50}	7	7
w_2	4.3	3.8	w_{50}	3.2	3.3
L_{2a}	19.6	19	r_1	4	4
L_{2b}	5.4	4.5	C_1	1.6 pF	1.5 pF
L_{2c}	14.3	12.6			

measured results of the proposed filtering CL-TRD coupler. The measured results are consistent with the simulated ones. It is observed that under the criterion of $|S_{11}| < -10$ dB, the BPBW range is 1.97 GHz \sim 2.97 GHz. Within the passband, $|S_{21}|$ is below -13 dB. From 2.02 GHz to 2.89 GHz, the AP imbalance is 3.2 ± 0.8 dB. From 1.93 GHz to 2.93 GHz, the phase difference is within $90^\circ \pm 5^\circ$. Besides, two stopbands from 0.91 GHz \sim 1.89 GHz and 3.36 GHz \sim 4.3 GHz are generated on two sides of the passband, respectively.

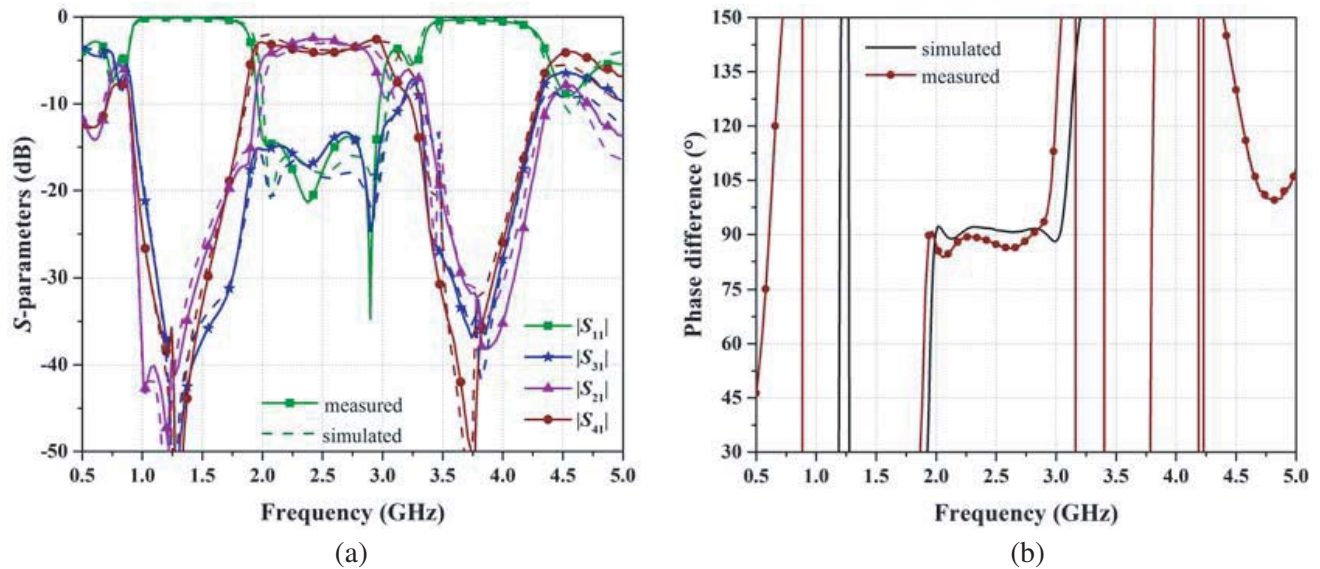


Figure 9. The simulated and measurement results of the prototype. (a) S -parameters. (b) Out ports phase differences.

Table 3 compares the measured results of the proposed filtering quadrature couplers with other related literatures. Compared with [6], the proposed filtering CL-TRD coupler shows wider BPBW. Although the BPBWs of couplers in [9, 12] are wider than the proposed structure, they have some disadvantages. For instance, since tight coupling coupled lines are used [9, 12], the fabrication of the gaps between the coupled lines is difficult. In the design, due to the insertion of capacitor, the odd-mode characteristic impedance can be chosen for realizing weak coupling, which effectively reduces the processing difficulty. Besides, the size of the proposed structure is smaller than the couplers in [9, 12]. The layout of the proposed structure is more flexible. In a comprehensive view, the proposed coupler is a good candidate for microwave applications.

Table 3. Comparison between the proposed filtering CL-TRD coupler with other quadrature filtering couplers.

Ref.	Type	Technique	Bandpass Relative Bandwidth (%)			Size ($\lambda_g \times \lambda_g$)
			$ S_{11} < 10$ dB	$ S_{21} < 10$ dB	PD = $90^\circ \pm 5^\circ$	
[6]	Filtering BL-COD coupler	Source-load coupling	4	1.7	–	0.185×0.106
[9]	Filtering BL-COD coupler	Tight coupling	60	60	53	0.89×0.69
[12]	Filtering power divider + phase shifter	Tight coupling	51	51	48	1.36×0.97
This work	Filtering CL-TRD coupler	Weak coupling	41.7	41.7	41.7	0.88×0.64

4. CONCLUSION

In the paper, a broadband filtering CL-TRD coupler has been proposed. The coupler consists of three coupled lines, four transmission lines, and four shunt stubs. The design equations of the proposed circuit are derived, and a prototype is designed, fabricated, and measured for validation. The measured results are in good coordination with the simulated ones. From the measured results, it is concluded that the proposed circuit can provide a broad BPBW, good isolation, flatten output ports amplitude and phase difference. Besides, two stopbands with sharp rejection are also achieved. Compared with the reported filtering quadrature couplers, the proposed structure shows wider bandwidth, smaller size, easier fabrication, and low cost.

ACKNOWLEDGMENT

This work was supported in part by the National Natural Science Foundation of China under Grant 51809030 and Grant 61871417, in part by the Natural Science Foundation of Liaoning Province under Grant 2020-MS-127, and in part by the Fundamental Research Funds for the Central Universities under Grant 3132020207 and Grant 3132020206.

REFERENCES

1. Chiu, J.-C., C.-M. Lin, and Y.-H. Wang, "A 3-dB quadrature coupler suitable for PCB circuit design," *IEEE Trans. Microw. Theory Techn.*, Vol. 54, No. 9, 3521–3525, Sep. 2006.
2. Tseng, C.-H. and Y.-T. Chen, "Design and implementation of new 3-dB quadrature couplers using PCB and silicon-based IPD technologies," *IEEE Transaction on Components, Packaging and Manufacturing Technology*, Vol. 6, No. 5, 675–682, May 2016.
3. Psychogiou, D., R. Gómez-García, and D. Peroulis, "RF wide-band bandpass filter with dynamic in-band multi-interference suppression capability," *IEEE Transactions on Circuits and Systems — II: Express Briefs*, Vol. 65, No. 7, 898–902, Jul. 2018.

4. Wu, X., Y. Li, and X. Liu, "High-order dual-port quasi-absorptive microstrip coupled-line bandpass filters," *IEEE Trans. Microw. Theory Techn.*, Vol. 68, No. 4, 1462–1475, Apr. 2020.
5. Chen, C.-F., T.-Y. Huang, C.-C. Chen, et al., "A compact filtering rat-race coupler using dual-mode stub-loaded resonators," *IEEE MTT-S International Microwave Symposium Digest*, 2012.
6. Lin, T.-W., J.-Y. Wu, and J.-T. Kuo, "Compact filtering branch-line coupler with source-load coupling," *IEEE International Workshop on Electromagnetics: Applications and Student Innovation Competition (iWEM)*, 2016.
7. Xiang, B. and S. Zheng, "Bandpass filtering 180° patch coupler with wide suppression band," *IEEE 5th Asia-Pacific Conference on Antennas and Propagation (APCAP)*, WE3A-13, 97–98, 2016.
8. Shao, Q., F.-C. Chen, Q.-X. Chu, et al., "Novel filtering 180° hybrid coupler and its application to 2 × 4 filtering butler matrix," *IEEE Trans. Microw. Theory Techn.*, Vol. 66, No. 7, 3288–3296, Jul. 2018.
9. Wong, Y. S., S. Y. Zheng, and W. S. Chan, "A wideband coupler with wide suppression band using coupled stub," *Proceedings of the Asia-Pacific Microwave Conference*, 1058–1061, 2011.
10. Chou, P.-J., C.-C. Yang, and C.-Y. Chang, "Exact synthesis of unequal power division filtering rat-race ring couplers," *IEEE Trans. Microw. Theory Techn.*, Vol. 66, No. 7, 3277–3287, Jul. 2018.
11. Gómez-García, R., J.-M. Muñoz-Ferreras, and D. Psychogiou, "Input-reflectionless out-of-phase 3-dB bandpass filtering couplers," *IEEE Radio and Wireless Symposium (RWS)*, 2019.
12. Wang, W. M., Y. Zheng, Y. L. Wu, et al., "Wide-band filtering three-port coupler with inherent DC-blocking function," *IEEE Access*, Vol. 7, 13170–13177, Feb. 2019.
13. Gómez-García, R., L. Yang, J.-M. Muñoz-Ferreras, et al., "Single/Multi-band coupled-multi-line filtering section and its application to RF diplexers, bandpass/bandstop filters, and filtering couplers," *IEEE Trans. Microw. Theory Techn.*, Vol. 67, No. 10, 3959–3972, Oct. 2019.
14. Dong, G., W. Wang, Y. Wu, et al., "Filtering rat-race couplers with impedance transforming characteristics based on terminated coupled line structures," *IET Microwaves, Antennas & Propagation*, Vol. 14, No. 8, 732–742, Mar. 2020.
15. Yum, W., Y. Rao, H. Jenny Qian, et al., "Reflectionless filtering 90° coupler using stacked cross coupled-line and loaded cross-stub," *IEEE Microwave and Wireless Components Letters*, Vol. 30, No. 5, 481–484, May 2020.
16. Shie, C.-I., J.-C. Cheng, S.-C. Chou, et al., "Transdirectional coupled-line couplers implemented by periodical shunt capacitors," *IEEE Trans. Microw. Theory Techn.*, Vol. 57, No. 12, 2981–2987, Dec. 2009.
17. Pozar, D. M., *Microwave Engineering*, 4th edition, John Wiley & Sons, Inc., New York, 2011.